Clin Pharmacokinet (2017) 56:925–939
DOI 10.1007/s40262-016-0484-2

ORIGINAL RESEARCH ARTICLE

Translational Modeling and Simulation in Supporting Early-Phase Clinical Development of New Drug: A Learn–Research–Confirm Process

Dongyang Liu[1] · Yi Zhang[2] · Ji Jiang[1] · John Choi[2] · Xuening Li[3] · Dalong Zhu[4] · Dawei Xiao[5] · Yanhua Ding[6] · Hongwei Fan[7] · Li Chen[2] · Pei Hu[1]

Published online: 20 December 2016
© Springer International Publishing Switzerland 2016

Abstract

Background and Objective Pharmacokinetic/pharmacodynamic modeling and simulation can aid clinical drug development by dynamically integrating key system- and drug-specific information into predictive profiles. In this study, we propose a methodology to predict pharmacokinetic/pharmacodynamic profiles of sinogliatin (HMS-5552, RO-5305552), a novel glucokinase activator to treat diabetes mellitus, for first-in-patient (FIP) studies.

Methods and Results Initially, pharmacokinetic/pharmacodynamic profiles of sinogliatin and another glucokinase activator (US2) previously acquired from healthy subjects were fitted using Model A incorporating an indirect response mechanism. The pharmacokinetic/pharmacodynamic profiles of US2 in patients with type 2 diabetes mellitus (T2DM) were then fitted using Model B incorporating circadian rhythm and food effects after thoughtful research on the difference between healthy subjects and T2DM patients. The differences in results between the two US2 modeling populations were used to scale the values of the pharmacodynamic parameters and refine the pharmacodynamic model of sinogliatin, which was then utilized to project pharmacokinetic/pharmacodynamic profiles of sinogliatin in T2DM patients after an 8-day simulated treatment. Results showed that the projected pharmacokinetic/pharmacodynamic values of five parameters were within 70–130% of values fitted from observed clinical data while the other two remaining projected parameters were within a twofold error. Population pharmacokinetic/pharmacodynamic analysis conducted for sinogliatin also suggested that age and sex were significantly correlated to pharmacokinetic/pharmacodynamic characteristics. Additionally, Model B was combined with a glycosylated hemoglobin (HbA_{1c}) compartment to form Model C, which was then used to project serum HbA_{1c} levels in patients after a 1-month simulated treatment of sinogliatin. The predicted HbA_{1c} changes were nearly identical to observed clinical values (0.82 vs. 0.78%).

Conclusions Model-based drug development methods utilizing a learn–research–confirm cycle may accurately project pharmacokinetic/pharmacodynamic profiles of new drugs in FIP studies.

Electronic supplementary material The online version of this article (doi:10.1007/s40262-016-0484-2) contains supplementary material, which is available to authorized users.

✉ Pei Hu
pei.hu.pumc@gmail.com

1 Clinical Pharmacology Research Center, Peking Union Medical College Hospital and Chinese Academy of Medical Sciences, Beijing 100032, China

2 HuaMedicine (Shanghai) Ltd., Shanghai, China

3 Department of Clinical Pharmacology, Zhongshan Hospital, Fudan University, Shanghai, China

4 Department of Endocrinology, DrumTower Hospital Affiliated to Nanjing University Medical School, Nanjing, China

5 Department of Clinical Pharmacology, First Hospital of Nanjing Medical University, Nanjing, China

6 Phase I Clinical Trial Unit, China-Frontage USA, The First Hospital of Jilin UniversityJilin University, Changchun, China

7 Department of Clinical Pharmacology, Nanjing First Hospital Affiliated to Nanjin Medical University, Nanjing, China

Key Points

We provide good validated example of learn–research–confirm methodology to show how to predict pharmacokinetics/pharmacodynamics in patients with complex system profiles based on data from healthy subjects.

The results of the population pharmacokinetic/pharmacodynamic analysis offered an insightful basis for further modeling research of sinogliatin (HMS-5552, RO-5305552), a novel glucose kinase activator, during future phase II/III trials.

1 Introduction

Accurately predicting pharmacokinetic/pharmacodynamic profiles of a new drug in first-in-patient (FIP) studies by analyzing the pharmacokinetic/pharmacodynamic characteristics in healthy subjects could greatly support clinical pharmacologists in trial design by, for example, optimizing dose selection or setting inclusion/exclusion criteria. However, making such predictions is challenging because of potentially different modulation systems and drug potency between healthy subjects and patients. To better quantitatively understand these differences, modeling and simulation was considered useful in integrating key system- and drug-specific information in the recent two decades [1–3]. However, only a few cases have been reported [4, 5] and validated so far.

Glucokinase (GK) is a key enzyme that phosphorylates D-glucose to glucose-6-phosphate, which is the first step of glucose metabolism in cells [6]. It serves as a 'glucose sensor' to regulate glucose-stimulated insulin release in pancreatic β cells. It also serves as glucose translator to convert glucose to glycogen and regulates glucose production in liver [6, 7]. The differential regulation function in pancreatic islets and liver allows GK activators (GKAs) to improve insulin secretion caused by both β cell dysfunction and insulin resistance, the two key characteristics of type 2 diabetes mellitus (T2DM) pathology. Therefore, GKAs represent a promising new class of drugs to treat T2DM [8]. Sinogliatin (HMS-5552, RO-5305552) is a fourth-generation GKA with a structurally novel amino acid-based chemical scaffold. Preclinical experiments suggested that sinogliatin is a potent and safe drug candidate to treat diabetes, and prior to the present study a single ascending dose (SAD) study was conducted to evaluate its safety, tolerability, pharmacokinetics, and pharmacodynamics following oral administration in healthy subjects [9]. This SAD study showed that sinogliatin significantly decreased fasting serum glucose (FSG) by up to 1.2 mmol/L at the maximum tested dose of 50 mg in healthy subjects. Because diabetic patients will have higher fasting and 24-h glucose baselines, the clinically effective dose should theoretically be higher than 50 mg in T2DM patients. Hence, simulating the pharmacokinetic/pharmacodynamic characteristics for these T2DM patients in order to optimize the dose would be especially valuable for accelerating the clinical development of sinogliatin.

Here, we propose a methodology to translate pharmacokinetic/pharmacodynamic characteristics from healthy subjects to diabetic patients using a novel GKA, sinogliatin, as an example. The specific objectives of the present study are to (1) predict FSG profiles in diabetic patients after a simulated 8-day dosing of sinogliatin on the basis of pharmacokinetic/pharmacodynamic characteristics of sinogliatin in healthy subjects and another same-in-class GKA (US2) in both healthy subjects and diabetic patients; (2) quantitatively address the key factors affecting pharmacokinetic/pharmacodynamic characteristics of sinogliatin in diabetic patients; and (3) predict glycosylated hemoglobin (HbA_{1c}) dynamics in diabetic patients after 1-month dosing of sinogliatin. We hope this will offer a useful example to project pharmacokinetic/pharmacodynamic profiles in patients with complex system on the basis of data in healthy subjects, especially for drugs of the same class as GKA. Additionally, the results of the population pharmacokinetic/pharmacodynamic analysis could offer a solid basis for further modeling research on sinogliatin during future phase II/III trials.

2 Methods

2.1 Study Design

Data were obtained from five studies: (1) a SAD study of sinogliatin in healthy subjects; (2) a SAD study of US2 in healthy subjects; (3) an 8-day multiple ascending dose (MAD) study of US2 in diabetic patients; (4) an 8-day MAD study of sinogliatin in diabetic patients; and (5) a 1-month MAD study of sinogliatin in diabetic patients (Table 1). In studies 1–4, plasma drug concentrations and FSG levels were determined via intensive sampling. In study 5, HbA_{1c} was additionally measured. The overall prediction strategy is summarized in Fig. 1. Firstly, pharmacokinetic/pharmacodynamic profiles of sinogliatin in T2DM patients were predicted based on pharmacokinetic/pharmacodynamic modeling results of sinogliatin in healthy subjects by translational borrowing of quantitative differences in pharmacokinetic/pharmacodynamic characteristics of US2 between healthy subjects and T2DM patients. The differences in pharmacokinetic/

Table 1 Summary of clinical studies

	Study number				
	1	2	3	4	5
Investigational drug	Sinogliatin	US2	US2	Sinogliatin	Sinogliatin
Phase	Ia	Ia	Ib	Ib	Ic
Administration	Single dose	Single dose	Single dose followed by 6-day continuous doses (bid) starting on Day 3		28-day doses (bid)
Dose level (number) (mg)[a]	0 (12), 5 (8), 10 (8), 15 (8), 25 (8), 35 (8), 50 (8)	0 (6), 5 (9), 10 (10), 25 (10)	0 (12), 10 (8), 25 (8), 50 (8), 100 (8), 200 (7)[b]	0 (10), 25 (8), 50 (10), 100 (10), 150 (8), 200 (7)	75 (12)[b]
Volunteers	Healthy subjects	Healthy subjects	T2DM patients	T2DM patients	T2DM patients
Co-administration	No	No	No	No	No
Placebo effect modeled	No	No	Yes	Yes	No
Food status at the time of drug administration[c]	Fasted	Fasted	Fed on Days 1 and 7, fasted on Days 3 and 8	Fed on Days 1 and 7, fasted on Days 3 and 8	Fed
PK/PD measurements	Plasma drug concentration, serum glucose, insulin, glucagon, C-peptide, GLP-1 concentrations	Plasma drug concentration, serum glucose, insulin, glucagon, C-peptide, GLP-1 concentrations	Plasma drug concentration, serum glucose, insulin, glucagon, C-peptide, GLP-1 concentrations	Plasma drug concentration, serum glucose, insulin, glucagon, C-peptide, GLP-1 concentrations	Plasma drug concentration, serum glucose, insulin, glucagon, C-peptide, GLP-1, HbA_{1c} concentrations
PK sampling time	Days 1–3 (0, 0.25, 0.5, 1, 1.5, 2, 2.5, 3, 4, 5, 6, 8, 12, 16, 24, 48, 72 h)	Days 1–2 (0, 0.25, 0.5, 1, 1.5, 2, 3, 4, 6, 8, 12, 16, 24, 36, 48 h)	Days 1, 3, and 8 (0, 0.25, 0.5, 1, 1.5, 2, 3, 4, 6, 8, 12, 16, 24, 36, 48 h)[d]	Days 1, 3, 7, and 8 (0, 0.25, 0.5, 1, 1.5, 2, 3, 4, 6, 8, 12, 16, 24, 36, 48 h)[e]	Not applied to the current study
PD sampling time	Day 1 (0, 0.25, 0.5, 1, 2, 3, 4 h)	Day 1 (0, 0.33, 0.67, 1, 1.33, 1.67, 2, 2.33, 2.67, 3, 3.33, 3.67, 4 h)	Days 1, 3, and 8 (0, 0.5, 1, 1.5, 2, 2.5, 3, 3.5, 4, 24, 48 h); Days 4, 5, 6, and 7 (0 h)	Days 1, 3, 7, and 8 (0, 0.5, 1, 1.5, 2, 3, 4, 24, 48 h)[f], Days 4, 5, 6 (0 h)	Days 1, 14, 28 (0 h)[g]

bid twice daily, *GLP-1* glucagon-like peptide-1, HbA_{1c} glycosylated hemoglobin, *PD* pharmacodynamic, *PK* pharmacokinetic, *T2DM* type 2 diabetes mellitus

[a] 0 means placebo group

[b] Also dosed as once daily

[c] For fasted status, fasted status was kept for 10 h before dosing and 4 h after dosing. For study in T2DM patients, fed status means drug was administered 1 h before meal and meal should be finished within 30 min

[d] 0–12 h for Day 3

[e] 0–12 h for Days 3 and 7

[f] 0–4 h for Days 3 and 7

[g] Sampling time for HbA_{1c}. Other PD biomarkers were not applied to the current study and, therefore, not reported here

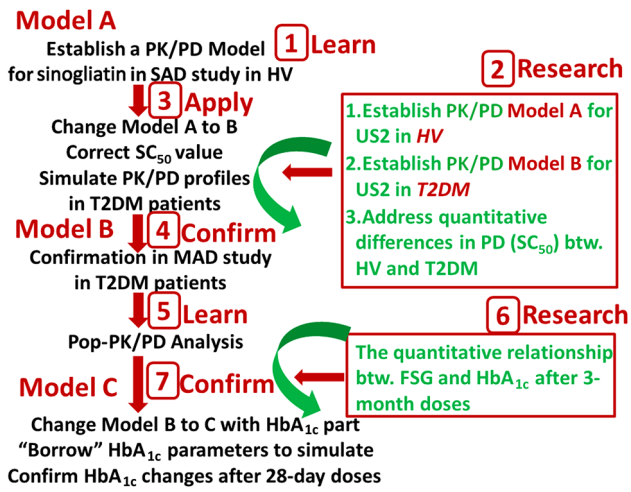

Fig. 1 The overall prediction strategy. *btw* between, *FSG* fasting serum glucose, *HbA$_{1c}$* glycosylated hemoglobin, *HMS5552* sinogliatin (RO-5305552), *HV* healthy volunteers, *MAD* multiple ascending dose, *PD* pharmacodynamics, *PKPD* pharmacokinetic/pharmacodynamic, *Pop-PKPD* population pharmacokinetic/pharmacodynamic, *SAD* single ascending dose, *SC$_{50}$* drug concentration in the central compartment at which the stimulation effect is half of the maximum effect of glucokinase on plasma glucose, *T2DM* type 2 diabetes mellitus

pharmacodynamic characteristics between the two populations were assumed to be same for both sinogliatin and US2. Because of systemic differences between the two populations, Model A and B were developed to mimic pharmacokinetic/pharmacodynamic profiles of GKA in healthy subjects and T2DM patients, respectively. This translational prediction was validated with observed pharmacokinetic/pharmacodynamic profiles of sinogliatin in T2DM patients, which were further analyzed using a nonlinear mixed-effect modeling method to quantify the key factors affecting pharmacokinetic/pharmacodynamic profiles of inogliatin in T2DM patients. Finally, serum HbA$_{1c}$ levels in patients after 1-month treatment of sinogliatin were simulated by assuming that the quantitative relationship between serum glucose (SG) and HbA$_{1c}$ was the same as previously reported in the literature. This simulation was also validated using observed HbA$_{1c}$ profiles after later sinogliatin treatment.

2.2 Prediction of Pharmacokinetic/Pharmacodynamic Characteristics for Sinogliatin from Healthy Subjects to Patients with Diabetes

2.2.1 Modeling Analysis of Pharmacokinetic/Pharmacodynamic Profiles of sinogliatin and US2 in Healthy Subjects

Mean concentration–time profiles across all dose levels were simultaneously fitted using the ADAPT5 package

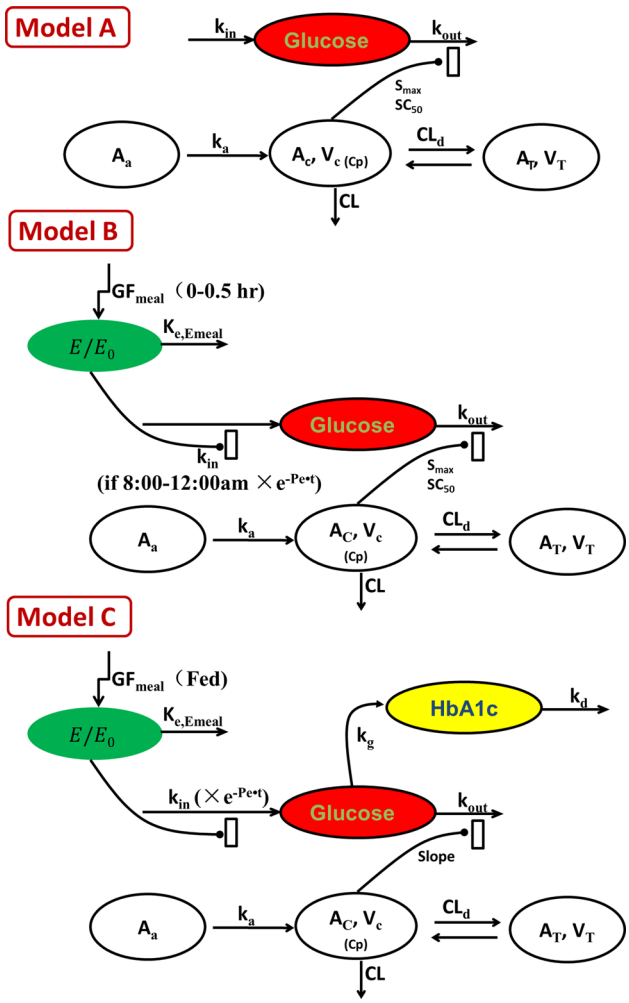

Fig. 2 The proposed model structures for Models *A*, *B*, and *C*. *A$_a$* drug amount in absorption compartment, *CL* systemic clearance, *CL$_d$* distribution clearance between the central and peripheral compartments, *E/E$_0$* relative food effect, *GF$_{meal}$* total food effect on production of glucose, *k$_a$* absorption rate constant, *k$_d$* elimination rate constant of serum HbA$_{1c}$, *k$_{e,Emeal}$* elimination rate constant of *E/E$_0$*, *k$_{out}$* turnover rate constant of plasma glucose, *SC$_{50}$* drug concentration in the central compartment at which the stimulation effect is half *S$_{max}$*, *S$_{max}$* maximum effect of glucokinase on plasma glucose, *V$_T$* distribution volume of the peripheral compartment, K$_{in}$ production rate constant of plasma glucose, A$_c$ drug amount in central compartment, A$_T$ drug amount in tissue compartment, V$_c$(C$_p$) distribution volume of central compartment (plasma drug concentration in central compartment), e$^{pe.t}$ decrease function of plasma glucose in the morning in T2DM patients, k$_g$ transduction rate constant from plasma glucose to HbA1c

(Biomedical Simulations Resource, Los Angeles, CA, USA) [10]. A two-compartmental pharmacokinetic model (Eqs. 1–3) with linear clearance and absorption was utilized to fit pharmacokinetic profiles for each drug of sinogliatin and US2 in healthy subjects. An indirect response model (IDR) with stimulation of response elimination (Eq. 4) was utilized to fit mean FSG–time profiles of each drug in healthy subjects due to the mechanism of

action for GKA [6]. The applied pharmacokinetic/pharmacodynamic model (Model A; see Fig. 2a) was selected according to the F test ($\alpha = 0.05$) of the Akaike Information Criterion value, precision of estimated parameters, and overall goodness-of-fit. Their residual unexplained variabilities (RUV) were described by a proportional error model (Eq. 5).

$$V_p \frac{dC_p}{dt} = k_a \cdot A_a - CL \cdot C_p - CL_d(C_p - C_t) \quad C_p(0) = 0 \tag{1}$$

$$V_t \frac{dC_t}{dt} = CL_d(C_p - C_t) \quad C_t(0) = 0 \tag{2}$$

$$\frac{dA_a}{dt} = -k_a \cdot A_a \quad A_a(0) = 0 \tag{3}$$

$$\frac{dGlu}{dt} = G_{base} \cdot k_{out} - k_{out} \cdot Glu \cdot \left(1 + \frac{S_{max} \cdot C_p}{SC_{50} + C_p}\right) Glu(0) = G_{base} \tag{4}$$

$$Y_{obs} = Y_{pred} \times (1 + \varepsilon_1) \tag{5}$$

where C_p and C_t are the drug (sinogliatin or US2) concentrations in the central and peripheral compartments; V_p and V_t are the distribution volumes of drug in the central and peripheral compartments; CL and CL_d are the systemic clearance in the central compartment and the distribution clearance between the central and peripheral compartment of drug; k_a and A_a are the absorption rate constant and amount of drug in deposit compartment; Glu represents SG level and G_{base} is its baseline level; k_{out} is the turnover rate constant of plasma glucose, which actually reflect effects of insulin and glucagon as well as elimination rate constant of glucose; S_{max} is the maximum stimulation effect and SC_{50} is the drug concentration in the central compartment at which the stimulation effect is half S_{max}; Y_{obs} and Y_{pred} are the observed and predicted plasma concentrations; and ε_1 is the proportional component quantifying the residual error, being assumed to be normally distributed in the range from 0 to σ^2.

2.2.2 *Modeling Analysis of Pharmacokinetic/Pharmacodynamic Profiles of US2 in Patients with Diabetes*

Because US2 was orally administrated under both fasting and fed status in the 8-day MAD study, the meal effect on SG levels was additionally considered. In order to simplify modeling analysis, the relative food effect (E/E_0) with a fixed initial value of 1 was utilized to describe the food effect. Because food consumption was finished within 0.5 h, total food effect on production of glucose (GF_{Meal}) was assumed to be infused in the first 0.5 h after food intake with a rate constant of $GF_{Meal}/0.5$ [11]. Circadian rhythm was observed in T2DM patients in the placebo group, as reported by other groups [12, 13]. SG levels were measured at 0–4 h post-dose, which was 8:00 a.m.–12 noon. These measurements did not support a modeling analysis with a full circadian rhythm model describing 24-h profiles. Considering SG levels were reported to be gradually decreasing during this time, a simple exponential elimination function (Eq. 7) with an elimination rate constant of P_e (decrease rate constant of plasma glucose in the morning in T2DM patients) was utilized to mimic the circadian rhythm in the morning. During the rest of the day, the glucose level will return to the baseline value according to the characteristics of IDR model without consideration of food and drug effects. The feedback function [14] caused by sequential increased insulin was not considered because a minor feedback phenomenon was only observed at 1 h for the highest dose group, which didn't support the fitting of this mechanism for all groups. After integrating meal effect and circadian rhythm in the morning, Model A was modified to Model B (Fig. 2b, Eqs. 1–3 and 5–7), which was then utilized to fit pharmacokinetic/pharmacodynamic profiles of US2 in T2DM patients using the ADAPT5 package.

$$\frac{dE/E_0}{dt} = \frac{GF_{meal}}{0.5}(\text{if } 0\text{–}0.5 \text{ h}) + k_{e,Emeal} - k_{e,Emeal} \cdot \frac{E}{E_0} \quad \frac{E}{E_0}(0) = 1 \tag{6}$$

$$\frac{dGlu}{dt} = G_{base} \cdot k_{out} \cdot \frac{E}{E_0}(\cdot e^{-Pe \cdot T} \text{if in the morning}) - k_{out} \cdot Glu \cdot \left(1 + \frac{S_{max} \cdot C_p}{SC_{50} + C_p}\right) \quad Glu(0) = G_{base} \tag{7}$$

where E/E_0 represents the relative effect of the meal; GF_{meal} reflects the total amount of meal effect and $k_{e,Emeal}$ is the elimination rate constant of E/E_0; and P_e represents the decrease rate constant of SG level of T2DM patients in the morning (8:00 a.m.–12 noon) due to the circadian rhythm.

2.2.3 *Extrapolation and Confirmation of Predicting Pharmacokinetic/pharmacodynamic Characteristics of Sinogliatin from Healthy Subjects to Diabetic Patients*

Model B was utilized to simulate pharmacokinetic/pharmacodynamic profiles of sinogliatin in T2DM patients. The values of sinogliatin pharmacokinetic parameters in T2DM patients were assumed to be the same as those in healthy

subjects. The food effect on pharmacokinetic profiles of sinogliatin in T2DM patients was assumed to be negligible due to (1) no potential mechanisms to produce differences between the two populations [5]; and (2) its two absorption characteristics: high bioavailability in dogs (89.4%), and high permeability (1.7 μm/s from the apical to basolateral side [15]) (unpublished data). Pharmacodynamic parameters of sinogliatin, G_{base}, k_{out}, S_{max}, and SC_{50}, in patients were scaled on the basis of their differences in US2 between healthy subjects and T2DM patients. The other three pharmacodynamic parameters, GF_{meal}, $k_{e,Emeal}$, and P_e, were assumed to be the same between studies 3 and 4 since the same food composition was consumed in both studies and these system parameters are not expected to change significantly in T2DM patients. After study 4 was conducted for sinogliatin, the pharmacokinetic/pharmacodynamic parameters were simultaneously estimated based on Model B using the ADAPT5 package and their values were compared with the parameter values used to simulate pharmacokinetic/pharmacodynamic profiles in patients in order to assess predictive accuracy of the current methodology.

2.3 Population Pharmacokinetic/pharmacodynamic Analysis of Sinogliatin in Patients with Diabetes

For drug concentrations and plasma glucose levels in study 4 (Table 1), population pharmacokinetic/pharmacodynamic analysis was sequentially conducted with a nonlinear mixed-effect modeling approach, using NONMEM® version 7.2 software (ICON Development Solutions, Gaithersburg, MD, USA) interfaced with Pirana® (version 2.8.0, Pirana Software & Consulting BV, Amsterdam, The Netherlands). One- and two-compartmental pharmacokinetic models with linear elimination and absorption were assessed based on objective function value (OFV), goodness-of-fit, the precision of parameter estimates, diagnostic plots, and determination of physiological/pathological plausibility. The first-order conditional estimation with interaction (FOCEI) method was used to assess the parameters. Inter-individual variability (IIV) was assumed to be log-normally distributed and was described by an exponential model (Eq. 8). The RUV was described using a mixed-error model (Eq. 9).

$$P_{ij} = \theta_i \times \exp(\eta_{ij}) \quad (8)$$

$$Y_{obs} = Y_{pred} \times (1 + \varepsilon_1) \quad (9)$$

In Eq. 8, θ_i is the typical value of the ith population parameter; P_{ij} is the estimate of the ith parameter in the jth individual; and η_{ij} quantifies the deviation of the typical parameter value from the individual parameter value, assuming that η_{ij} is normally distributed in the range from 0 to ω^2. In Eq. 9, Y_{obs} and Y_{pred} are the observed and predicted plasma concentrations; ε_1 is the proportional component quantifying the residual error, being assumed to be normally distributed in the range from 0 to σ^2.

The pharmacokinetic/pharmacodynamic characteristics of sinogliatin were also described by Model B (Fig. 2b) with a modification replacing S_{max} and SC_{50} with the parameter slope, which means the maximum effect (Emax) model in Eq. 7 was replaced by slope·C_p. The following covariates were plotted against individual pharmacokinetic parameters: demographic population characteristics (body surface area [16], lean body weight [17], total body weight, age), body mass index (BMI), height, sex, liver function (alanine aminotransferase, aspartate transaminase, protein binding factor [albumin], and total bilirubin), and renal function (serum creatinine). The following covariates were plotted against individual pharmacodynamic parameters: BMI, age, sex, total cholesterol, high-density lipoprotein cholesterol, low-density lipoprotein cholesterol, fasted serum C-peptide, FSG, and fasted serum insulin. Considering the eta-shrinkage, these plots were utilized to guide the shape of the parameter-covariate relationships (e.g., linear or power) as well as to identify covariate relationships to be explored within NONMEM®. Covariates with a coefficient of determination value of higher than 0.3 were investigated in NONMEM® using stepwise forward inclusion ($P < 0.05$) and backward elimination ($P < 0.05$), guided by the difference in OFV. Power and linear covariate effects on pharmacokinetic parameters were tested for continuous variables (Eq. 10) and categorical variables (Eq. 11).

$$P_{ij} = \theta_1 \times \exp(\eta_{ij}) \times (X/X_{median})^{\theta} \quad (10)$$

$$P_{ij} = \theta_1 \times \exp(\eta_{ij}) \times (1 + \theta_2 \times X_{indicator}) \quad (11)$$

In Eq. 10, X is the individual covariate value and X_{median} is the median value of the jth covariate; And θ_1 is an estimate of the typical population parameter and θ_2 describes the effect of the covariate on P_{ij}. In Eq. 11, $X_{indicator}$ indicates the categorical covariate; and θ_2 describes the extent of the covariate effect.

Internal model evaluation during the population pharmacokinetic/pharmacodynamic (PopPK/PD) model-finding steps included assessments of decrease in OFV, precision of estimated parameters, inspection of goodness-of-fit plots from the basic model without inclusion of covariates and of the different covariate models, as well as graphical inspection of the relative standard error (RSE) of the mean by plotting the conditional weighted residuals over time after dose. In addition, the final PopPK/PD model was assessed using visual predictive checks (VPCs; $n = 500$) and non-parametric bootstrapping ($n = 500$). The VPCs were created with the Perl-speaks-NONMEM (PsN) toolkit

(version 3.6.2) [18] and Xpose (version 4.2.1) [19] for graphical analysis. A total of 500 datasets were sampled randomly from the original dataset, followed by fitting using the PsN toolkit (version 3.6.2) [18, 20].

2.4 Prediction of Pharmacokinetic/Pharmacodynamic Profiles of Sinogliatin after 28-Day Treatment in Study 5

An additional HbA_{1c} compartment was added into Model C with a transduction parameter (k_g) between SG and HbA_{1c} and the elimination rate constant of serum HbA_{1c} (k_d). k_d was borrowed from a publication (0.000664 1/h) and k_g was set to be equal to HbA_{1c} baseline $\times$ k_d/G_{base} [21]. This compartment was then utilized to simulate HbA_{1c} changes in T2DM patients with different baseline levels of FSG and HbA_{1c}, with additional information on variability in glucose changes estimated in the above PopPK/PD analysis. Clinical trial design for simulation was set as the final protocol of the real study. Other parameters were assumed to be the same as estimation in the above population analysis. The simulated HbA_{1c} changes from baseline were compared with observed value to evaluate predictive accuracy.

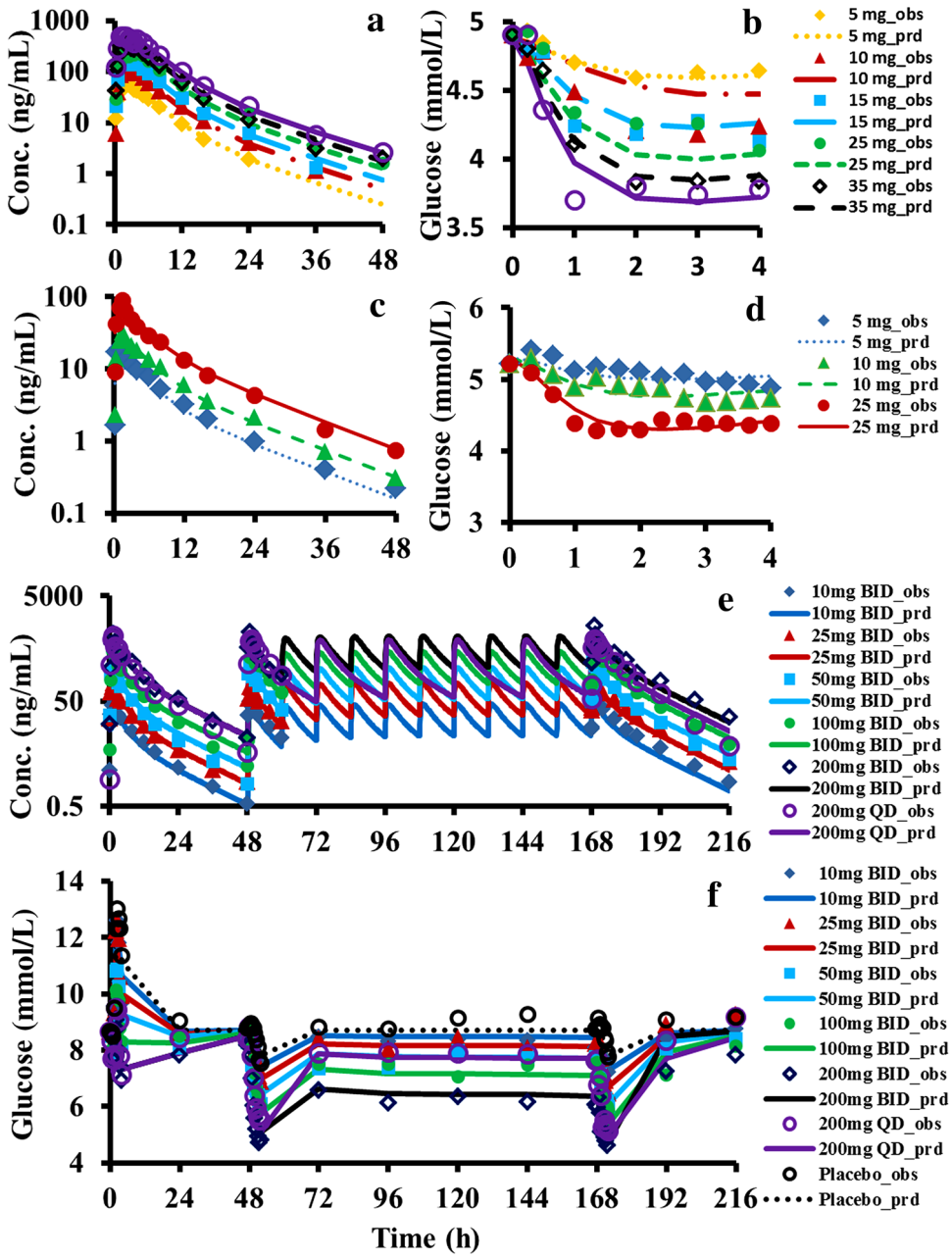

Fig. 3 Observed and fitted pharmacokinetic/pharmacodynamic profiles for sinogliatin (HMS-5552, RO-5305552) in healthy subjects and US2 in both healthy subjects and patients with type 2 diabetes mellitus. **a**, **b** Pharmacokinetic and pharmacodynamic profiles for sinogliatin in healthy subjects; **c**, **d** pharmacokinetic and pharmacodynamic profiles for US2 in healthy subjects; **e**, **f** pharmacokinetic and pharmacodynamic profiles for sinogliatin in patients with type 2 diabetes mellitus. *BID* twice daily, *Conc.* concentration, *obs* observed, *prd* predicted, *QD* once daily

3 Results

In this study, three sub-studies were conducted to project 8-day sinogliatin pharmacokinetic/pharmacodynamic profiles in diabetic patients from those in healthy subjects, quantify the key factors affecting sinogliatin pharmacokinetic/pharmacodynamic profiles in diabetic patients, and predict 28-day sinogliatin pharmacokinetic/pharmacodynamics in diabetic patients from those in 8-day sinogliatin treatment. These three sub-studies were conducted sequentially; therefore, their results are described below in the same order.

3.1 Predicting Pharmacokinetic/Pharmacodynamic Characteristics of Sinogliatin from Healthy Subjects to Diabetic Patients

3.1.1 Modeling Analysis of Pharmacokinetic/Pharmacodynamic Profiles for Sinogliatin in Healthy Subjects and US2 in Healthy Subjects and Type 2 Diabetes Mellitus Patients

Projected and observed pharmacokinetic/pharmacodynamic profiles for sinogliatin in healthy subjects and US2 in healthy subjects and T2DM patients are shown in Fig. 3; these profiles suggest that Model A captured the pharmacokinetic/pharmacodynamic characteristics of sinogliatin and US2 in healthy subjects without systemic bias. Observed glucose–time curves for the middle three dose levels (10, 15, and 25 mg) are overlapped, which was possibly caused by small sample size for each dose level. Therefore, the fitting based on dose-dependent efficacy is not perfect for the three dose levels. However, glucose–time curves for the highest two dose levels and the lowest dose level were fitted well, which could give good confidence in predicting pharmacodynamic profiles in T2DM patients and conquer the limitation of overlapping for the middle three dose levels. According to the above

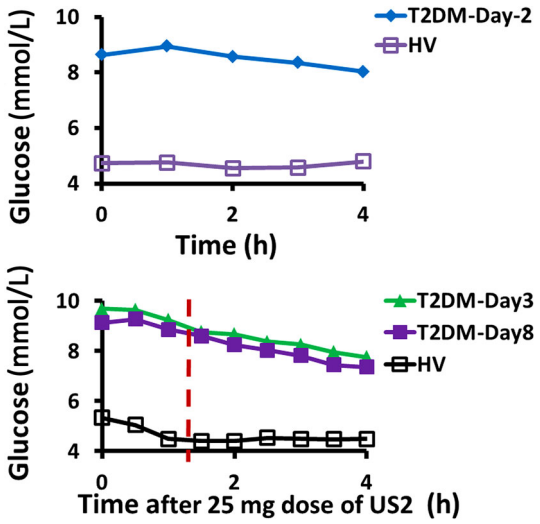

Fig. 4 Glucose–time curves in healthy subjects and patients with type 2 diabetes mellitus before (*upper*) and after (*lower*) administration of US2. *HV* healthy volunteers, *T2DM* type 2 diabetes mellitus

Table 2 Fitting results of pharmacokinetic/pharmacodynamic parameters for sinogliatin (HMS-5552, RO-5305552) in healthy subjects and US2 in both healthy subjects and patients with type 2 diabetes mellitus

Parameters	Description	Sinogliatin in healthy subjects		US2 in healthy subjects		US2 in T2DM patients	
		Estimate	CV%	Estimate	CV%	Estimate	CV%
CL (L/h)	Systemic clearance in the central compartment	12.3	2.0	42.75	4.6	34.2	2.2
V_p (L)	Distribution volume of the central compartment	23.1	16.5	43.62	38.5	33.9	18.7
CL_d (L/h)	Distribution clearance between the central and peripheral compartment	2.86	23.5	28.07	42.1	22.3	21.5
V_t (L)	Distribution volume of the peripheral compartment	28.2	9.9	230	15.8	213	8.0
k_a (1/h)	Absorption rate constant	0.261	13.7	0.282	30.1	0.264	14.3
k_{out} (1/h)	Turnover rate constant of plasma glucose	2.51	21.2	1.45	15.9	0.485	8.0
G_{base} (mmol/L)	Baseline level of glucose	4.88	0.9	5.32	0.7	8.72	0.5
S_{max} (units)	Maximum effect of glucokinase on plasma glucose	0.607	14.0	0.607	FIXED[a]	1.01	8.4
SC_{50} (ng/mL)	Drug concentration in the central compartment at which the stimulation effect is half S_{max}	417	9.1	102	9.6	478	14.9
GF_{Meal} (units)	Total food effect on production of glucose	NA	NA	NA	NA	2.15	10.9
$k_{e,Emeal}$ (1/h)	Elimination rate constant of food effect	NA	NA	NA	NA	1.39	10.6
P_e (1/h)	Decrease rate constant of plasma glucose in the morning in T2DM patients	NA	NA	NA	NA	0.0508	10.2

CV% percentage coefficient of variability, *NA* not applicable, *T2DM* type 2 diabetes mellitus

[a] Fixed as sinogliatin

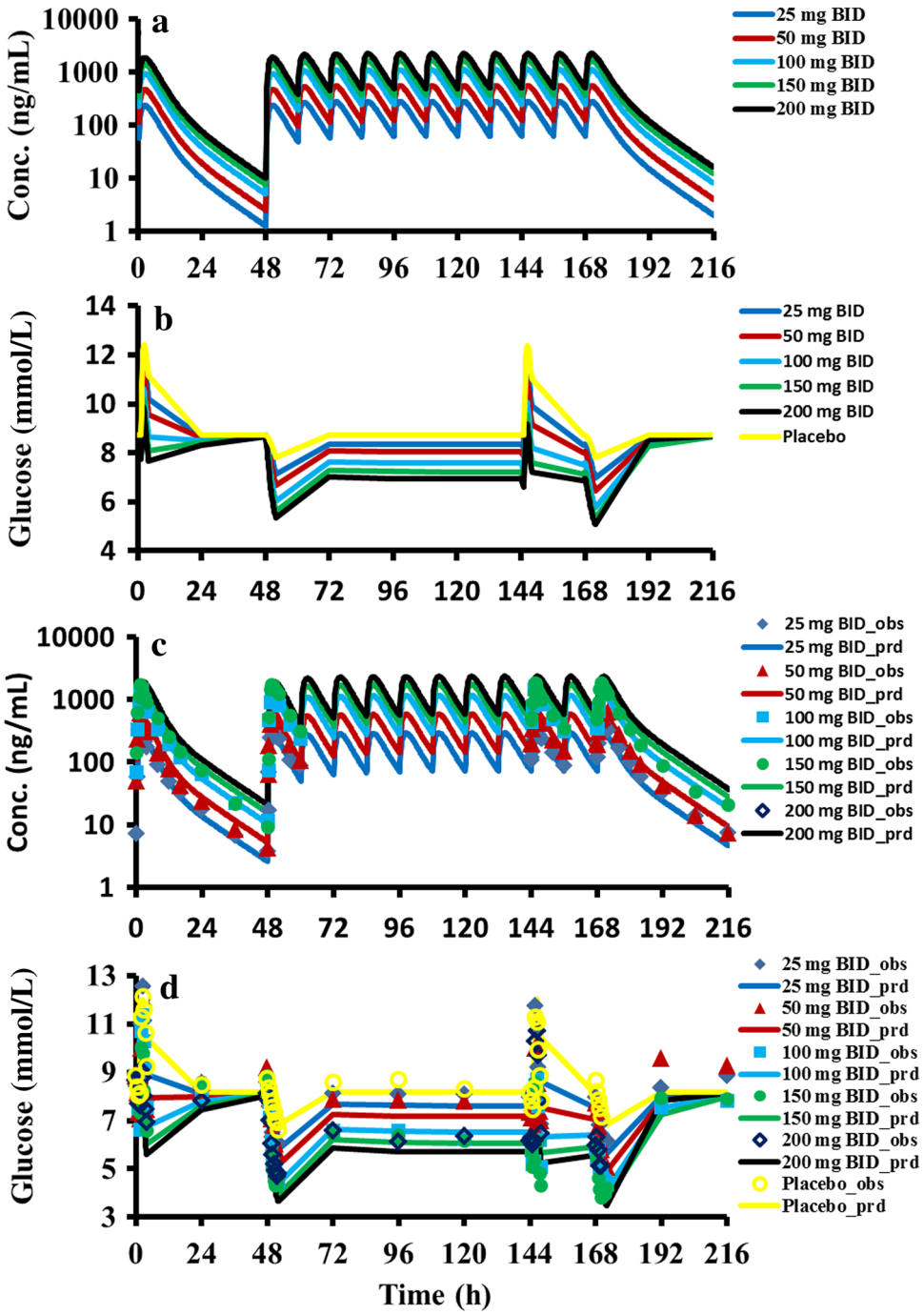

Fig. 5 Simulated and fitted pharmacokinetic/pharmacodynamic profiles of sinogliatin (HMS-5552, RO-5305552) in patients with type 2 diabetes mellitus after 8-day dosing. **a**, **b** Simulated pharmacokinetic and pharmacodynamic profiles of sinogliatin; **c**, **d** fitted pharmacokinetic and pharmacodynamic profiles of sinogliatin. *BID* twice daily, *Conc*. concentration, *obs* observed, *prd* predicted

understanding and research of glucose modulation in T2DM patients, Model A was modified to Model B, which was found to acceptably capture major pharmacokinetic/pharmacodynamic characteristics of US2 in T2DM patients (Fig. 3e, f). Additional figures with estimated and observed pharmacokinetic/pharmacodynamic profiles in T2DM patients are depicted in Electronic Supplementary Material 1A for each dose level. Estimated parameters are summarized in Table 2. The precisions expressed as the percentage coefficient of variability (CV%) were estimated to be less than 50% for all parameters, which showed robust estimation. In order to translate the systemic difference from US2 to sinogliatin under the same conditions, S_{max} was assumed to be same for both drugs in healthy subjects.

Table 3 Summary of values for simulation and fitted values of PK/PD parameters of sinogliatin (HMS-5552, RO-5305552) in T2DM patients based on data in healthy subjects

Parameter[a]	Simulation before study	Fitting after study	
	Projected values	Fitted values	CV%
CL (L/h)[b]	12.3	11.56	2.7
V_p (L)[b]	23.1	52.81	22.0
CL_d (L/h)[b]	2.86	3.72	28.9
V_t (L)[b]	28.2	37.27	15.8
k_a (1/h)[b]	0.261	0.5723	25.6
S_{max} (units)[c]	1.01	1.70	21.1
SC_{50} (ng/mL)[d]	1954	1970	31.8
G_{base} (mmol/L)[c]	8.72	8.19	1.2
k_{out} (1/h)[d]	0.828	0.614	15.9
GF_{Meal} (units)[c]	2.15	1.97	18.9
$k_{e,Emeal}$ (1/h)[c]	1.39	1.32	18.0
P_e (1/h)[c]	0.0508	0.0745	15.3

CV% percentage coefficient of variability, *T2DM* type 2 diabetes mellitus

[a] See Table 2 for definitions of parameters

[b] Simulated parameter value is obtained by estimation of sinogliatin in healthy subjects

[c] Simulated parameter value is the same as estimation of US2 in T2DM patients

[d] Simulated parameter value is scaled using the difference of this parameter of US2 between healthy subjects and T2DM patients

The smaller value of k_{out} in T2DM patients suggested a slower rate of return back to SG homeostasis than in healthy subjects, which could also be clearly observed by comparing drug effect in Fig. 4.

3.1.2 Extrapolation of Pharmacokinetic/Pharmacodynamic Characteristics of Sinogliatin from Healthy Subjects to Diabetic Patients

Simulated, observed, and fitted pharmacokinetic/pharmacodynamic profiles of sinogliatin in T2DM patients are depicted in Fig. 5 (separated figures for each dose level are depicted in Electronic Supplementary Material 1B) and summarized in Table 3. In a comparison of Fig. 5a, c, average plasma exposure expressed in area under the plasma concentration–time curve (AUC) and steady-state plasma drug concentration (C_{ss}), calculated using a non-compartment analysis method by Pheonix WinNonlin® 5.1 (Pharsight Co., Cary, NC, USA), was comparable (bias within ±10%), although an approximately twofold error existed in V_p and k_a between simulated and fitted values. In a comparison of Fig. 5b, d, similar trends were captured. In order to evaluate the predictive accuracy of drug effect in T2DM patients without interference from different baselines, projected/observed and fitted/observed values of glucose change from their baselines—time curves are depicted in Electronic Supplementary Material 1C and 1D. A decrease of 0.37–1.77 and 0.57–2.49 mmol/L of SG level was projected and fitted for sinogliatin at steady state over the dose range of 25–200 mg twice daily. The difference was caused by a higher value of the systemic parameter, S_{max} (1.01 vs. 1.70), in T2DM patients in study 4. The maximum glucose decrease after drug administration under a fasting state was projected and fitted to be –3.64 to –1.72 and –4.74 to –2.58 mmol/L. The small difference was caused by a bigger amplitude in the circadian rhythm, P_e (0.0508 vs. 0.0745 1/h), in T2DM patients. The relative peak value of the post-food glucose level at steady state (Day 7) was projected and fitted to be 0.428–2.81 and –1.32 to 2.34 mmol/L, which may be responsible for all of the differences in S_{max}, P_e, and k_{out}. In conclusion, the relative bias values were within the range of ±30% for five pharmacodynamic parameters but not for $S_{max}$and P_e, where relative bias within the range of ±70% was found between projected and fitted value.

3.2 Population Pharmacokinetic/Pharmacodynamic Analysis of Sinogliatin in Patients with Diabetes

A two-compartment model with linear absorption and elimination adequately captured the pharmacokinetic characteristics of sinogliatin in T2DM patients. The effects of IIV on CL, V_p, CL_d, and V_p and RUV of the model were best described using an exponential model and a proportional error model, respectively. Estimated PopPK/PD parameters are listed in Table 4. The precision of most parameters, expressed as a percentage RSE, was less than 50%, except for Ω_{CLD} (88.4%), Ω_{VT} (67.4%), and Ω_{slope} (52.7%), indicating that the model was fitted robustly. The effect of IIV on k_a tended towards 0, and was thus fixed at 0. CL was found to be inversely related to age (Eq. 12) (difference in OFV [ΔOFV] = 13; $P < 0.01$), which suggested that CL is decreased by ~30% when age is changed from 52 to 104 years. V_t was found to be smaller in females by 20% (Eq. 13) (ΔOFV = 7.6; $P < 0.05$). Renal or liver function have no significant effect on drug elimination, although the drug was majorly eliminated by the cytochrome P450 (CYP) 3A4 enzyme and ~10% of the dose was eliminated by the kidneys in parent drug.

$$CL = TVCL \times (AGE/52)^{-0.478} \quad (12)$$

$$V_t = TVVT\ (\times 0.8 \text{ if female}) \quad (13)$$

P_e was found to be 1.8 times in females than in males (Eq. 14) (ΔOFV = 8.4; $P < 0.01$), which suggested that FSG levels of female patients is decreased to a larger extent

Table 4 Population PK/PD analysis of sinogliatin (HMS-5552, RO-5305552) in T2DM patients with validation of bootstrap (n=500)

Parameters	Definition	Estimates	CV%	Bootstrap	IIV (%)	CV%	Bootstrap
CL (L/h)	Systemic clearance in the central compartment	12.2	4.0	[11.6, 12.8]	19.6	33.2	[15.6, 23.1]
V_p (L)	Distribution volume of the central compartment	32	29.7	[24.4, 39.5]	36.6	32.0	[28.2, 43.2]
CL_d (L/h)	Distribution clearance between the central and peripheral compartment	4.81	10.1	[3.82, 5.80]	29.2	88.4	[17.7, 52.0]
V_t (L)	Distribution volume of the peripheral compartment	43.5	10.0	[38.3, 48.6]	23.6	67.4	[15.3, 39.6]
k_a (1/h)	Absorption rate constant	0.374	26.1	[0.274, 0.474]	0 (FIXED)	NA	NA
Gender on V_t	Gender effect on V_t	–0.2	43.3	[–0.337, –0.0629]	NA	NA	NA
Age on CL	Age effect on CL	–0.478	48.6	[–0.847, –0.109]	NA	NA	NA
EPS	Residual error (CCV)	0.184	3.5	[0.167, 0.199]	NA	NA	NA
k_{out} (1/h)	Elimination rate constant for SG	0.617	10.4	[0.514, 0.759]	50	27.6	[35.9, 60.7]
G_{base} (mmol/L)	PG concentration at baseline	8.54	2.6	[8.15, 8.92]	19.6	19.3	[16.4, 22.5]
Slope [1/(μg/mL)]	Drug effect on decrease of PG	0.000587	12.6	[0.000465, 0.000720]	69.1	52.7	[44.6, 10.1]
$k_{,Emeal}$ (1/h)	Elimination rate constant for food effect on PG	0.86	10.3	[0.653, 1.04]	47	35.9	[28.2, 62.8]
GF_{Meal} (units)	Amount of food effect on PG	2.58	10.6	[2.13, 3.06]	39.9	27.1	[29.3, 48.0]
P_e (1/h)	Decrease rate constant for FSG in morning	0.054	12	[0.0355, 0.0701]	61.1	34	[42.7, 79.3]
Gender on P_e	Gender effect on P_e	0.823	34.1	[0.635, 2.20]	NA	NA	NA
Age on $k_{e,Emeal}$	Age effect on $k_{e,Emeal}$	–1.25	25.8	[–1.76, –0.32]	NA	NA	NA
IOV	Inter-day variability of food effect on PG	NA	NA	NA	45.9	18.9	[38.1, 58.5]
EPS	Residual error (CCV)	0.0131	3.5	[0.0115, 0.0147]	NA	NA	NA

CCV constant coefficient of variation, *CV%* percentage coefficient of variability, *FSG* fasting serum glucose, *NA* not applicable, *PG* plasma glucose, *SG* serum glucose

than in male patients when both are fasted. TVCL, TVVT, TVP_e, and $TVK_{e,Emeal}$ mean typical value of CL, V_T, P_e, and $K_{e,Emeal}$, respectively. $k_{e,Emeal}$ (the elimination rate constant of food effect) was found to be inversely related to age (Eq. 15) ($\Delta OFV = 6.1$; $P < 0.05$).

$$P_e = TVP_e(\times 1.8 \text{ if female}) \quad (14)$$

$$k_{e_Meal} = TVK_{e_Meal}(AGE/52)^{-1.25} \quad (15)$$

The fitting performance of the final PopPK/PD model is depicted in Electronic Supplementary Material 2 Figure 1. The scatter-plots of individual and population-predicted concentrations versus observed values showed no major bias, and most conditional weighted residuals were shown to lie within an acceptable range (−2 to 2). The pharmacokinetic/pharmacodynamic data for all treatment subgroups were simulated to form 500 datasets using the same experimental design and parameter estimates obtained with the FOCEI method. The 5th, 50th, and 95th percentiles (prediction intervals) of the simulated data were calculated and plotted as red lines against the observed concentrations, as shown in Electronic Supplementary Material 2 Figure 2. The model adequately predicted the observed data, with the prediction interval including most of the observed sinogliatin concentrations or FSG levels. The non-parametric stratified bootstrapping results fitted from 500 sampling datasets are shown in Table 4. The bootstrap analysis showed the original pharmacokinetic/pharmacodynamic model for sinogliatin concentrations/FSG levels to be stable and the estimated parameters to be precise.

3.3 Projection of Pharmacokinetic/pharmacodynamic Profiles of Sinogliatin after a 1-Month Treatment

Predicted HbA_{1c} percentage profiles are depicted in Fig. 6. The observed HbA_{1c} in T2DM patients after a 28-day treatment of sinogliatin 75 mg (twice daily) was observed to be decreased from 8.98 to 8.18%, which was predicted to be from 9.0 to 8.2%.

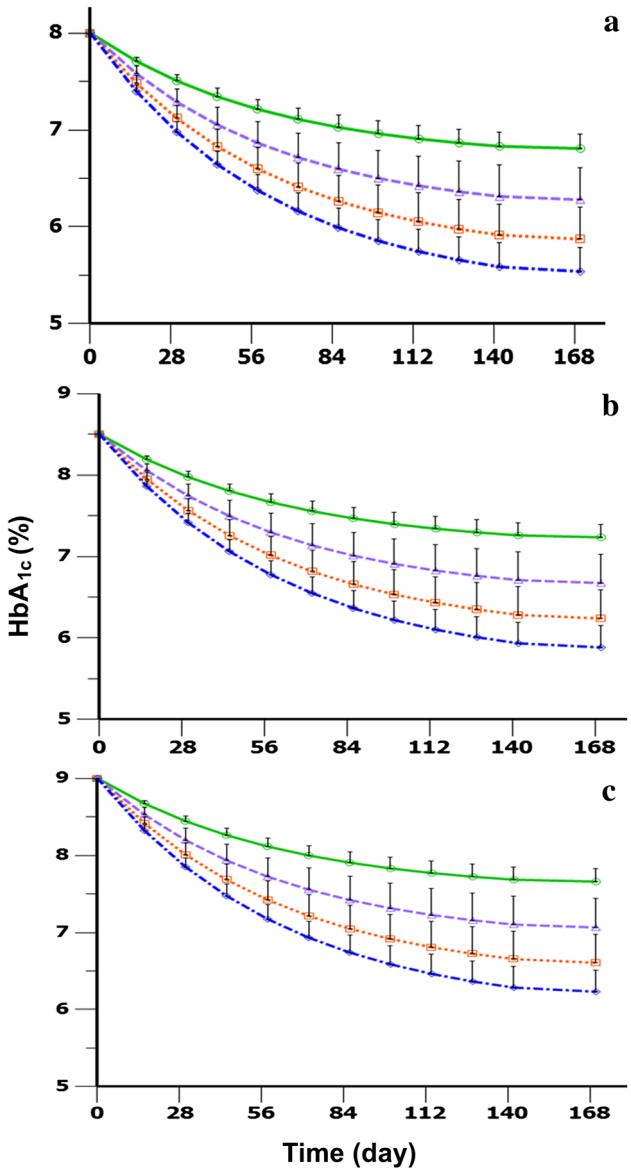

Fig. 6 Predicted glycosylated hemoglobin percentage profiles in patients with type 2 diabetes mellitus after dosing of sinogliatin (HMS-5552, RO-5305552) when the glycosylated hemoglobin baseline of patients with type 2 diabetes is 8% (**a**), 8.5% (**b**), and 9% (**c**). *HbA_{1c}* glycosylated hemoglobin

4 Discussion

Modeling and simulation have been extensively applied to predict pharmacokinetic/pharmacodynamic profiles of new drugs in new systems, such as from a preclinical study to a first-in-human (FIH) study [22, 23], from healthy subjects to patients [4, 5], and from a short-term treatment trial to a long-term treatment trial [24, 25]. Regarding pharmacokinetic prediction, physiologically based pharmacokinetic models have exhibited strong power in integrating specific system changes [26, 27]. For this kind of model, the prediction results could be reliable if key covariates are considered within the model. The system structure is known and we don't need to modify the model structure when we predict pharmacokinetic characteristics in new populations or species. However, we know much less about the pharmacodynamic system than the pharmacokinetic system. Therefore, many more challenges exist for accurate prediction of pharmacodynamic characteristics. So far, most studies translationally predicting pharmacodynamic profiles did not change the model structure by assuming the same modulation system between different populations. This did work for some drugs by either replacing a parameter value with the new system's value [22] or scaling the parameter using the difference between the two populations or species [23]. However, in most situations, significant differences exist between healthy subjects and patients. Therefore, in order to receive a reliable prediction, it is very important for us to identify the differences between systems as the first step. We then need to confirm these differences by searching the literature and understand the mechanism causing these differences. Next, we need to quantitatively describe this difference using reference drug data based on our understanding and its mechanism. Overall, it is a critical step to research the differences between systems before we make predictions, as this supports us to address, understand, and accurately quantify the system. Although several predictive studies have been conducted using data from healthy subjects for patients, few cases using modeling and simulation techniques have been reported and validated [4, 5]. In the present study, careful research was conducted, in which we modified the model structure based on the results of our research, and new mechanisms (circadian rhythm [12, 13] and food effect [11]) were addressed and confirmed from other studies. The following modeling research on reference drug, US2, revealed that drug-specific parameters (SC_{50} and S_{max}) and system-specific parameters (G_{base} and k_{out}) are significantly different between healthy subjects and T2DM patients. Additionally, incorporating circadian rhythm effects turned out to be necessary in modeling pharmacodynamic profiles of GKA in patients. Therefore, based on the research results, all of the above knowledge was dynamically integrated and quantitatively applied to predict pharmacokinetic/pharmacodynamic profiles of sinogliatin in T2DM patients based on the data generated from healthy subjects. This is our first learn–research–confirm cycle. The dynamic relationship between SG levels and HbA_{1c} has previously been reported in T2DM patients by other investigators [21]. Therefore, in the second cycle of learn–research–confirm, this previous learning was directly applied to assist in accurately predicting HbA_{1c} profiles of sinogliatin in T2DM patients by integrating variability estimated from a population pharmacokinetic/

pharmacodynamic study. The predictive performance of the two cycles of learn–research–confirm methodology proved to be successful, demonstrating the necessity of the 'research' step in the middle of 'learn' and 'confirm' if we would like to accurately predict pharmacokinetic/pharmacodynamic/disease profiles between different populations, especially populations with complex modulation systems.

So far, two kinds of pharmacodynamic model have been applied to GKA: one is a simple IDR model integrating the results of an in vitro study reported by Zager et al. [28] and the other is a complicated model integrating glucose, insulin, and glucagon characteristics reported by Schneck et al. [29]. In order to simplify glucose modulation, Zager et al. [28] grouped liver glycogen production, enhancement of insulin secretion, and peripheral effects into a basic IDR model structure using k_{in} and k_{out}. A huge turnover rate of plasma glucose (k_{out} = 5860 L/h) was estimated by Zager et al. [28] to show the elimination half-life of plasma glucose to be just ~0.4 s in mice, which is almost impossible. Although the pharmacodynamic model utilized by Schneck et al. [29] integrated more hormones, the fixed pharmacodynamic parameters (15 of 22 parameters) were 'borrowed' from a Caucasian population, which may not fit the aim of our study to predict pharmacodynamic profiles in a Chinese population. In order to predict pharmacodynamic profiles in a Chinese population accurately, we removed the in vitro part of the Zager et al. [28] model and utilized a standard IDR model to capture the entire modulation ofglucose. The parameter reflecting glucose metabolism, k_{out}, was estimated to be a rational value (0.485–2.51 1/h) and it was found to be lower in T2DM patients, which is consistent with other studies [30]. It was also found to be smaller in healthy Chinese subjects than it is in healthy Caucasian subjects; the reason for this has not been determined so far. Different BMIs (24.9 vs. 29.9 kg/m^2) may be one of the reasons as obese subjects will have weaker glucose control than normal subjects, which means a slower turnover rate [31].

It was suggested that the circadian rhythm of the SG level was caused by the changed rate of endogenous glucose production in patients, which is frequently high in the morning and decreases gradually to rates comparable with healthy subjects [30, 32, 33]. It exists in both T2DM patients and healthy subjects, but the extent of the fluctuation is six times stronger in patients than it is in healthy subjects [33]. Because the decrease in the morning was not observed in healthy subjects in the present study (Fig. 4), circadian rhythm was only considered in studies in T2DM patients, which is attributed to diurnal rhythm [32, 34]. The glucose level was estimated to be decreased by 20% ($=e^{-0.0508 \times 4\ h}$) in the morning, which is consistent with reported values in Caucasian T2DM patients [33, 35]. Interestingly, the glucose level decreases more in fasting Chinese T2DM patients with a higher P_e value (0.0745 1/h), which may be caused in different patient populations on the basis of different levels of endogenous glucose production between newly diagnosed and established T2DM patients [30]. The food effect on the glucose production rate constant was quantitatively described using a 0.5 h infusion function followed by an exponential decrease, which is similar to the measured glucose absorption rate in an oral meal tolerance test [36]. So far, a piece-wise model [37] and transit model [38] have been developed to fit the glucose absorption rate. However, the piece-wise model needs to estimate n - 1 parameters (where n is the sampling point number) while the transit model could not capture the profiles of a quick increase in a short time and a slow decrease during rest time. Therefore, we utilized the current model to mimic food effect on the glucose absorption rate. Population analysis suggested the P_e was 1.8 times higher in female than in male patients, which is newly reported here. The elimination rate constant of HbA_{1c} (k_d) was estimated to be 0.000664 L/h, which suggests a half-life of ~100 days. Due to HbA_{1c} being formed on the membrane of red blood cells, the half-life of HbA_{1c} is determined using the lifespan of red blood cells of 100–120 days [39]. This also reinforces the correct application of the k_d value in the second cycle of learn–research–confirm.

Sinogliatin is a novel GKA, which is undergoing early-phase clinical development. Neither pharmacokinetic/pharmacodynamic profiles nor pharmacokinetic/pharmacodynamic modeling analysis in patients have been reported so far. On the basis of its mechanism of action and its potent glucose-lowering efficacy, it is important to estimate optimal sinogliatin doses for T2DM patients [8, 40]. Therefore, real-time modeling and simulation would be helpful for sinogliatin in early-phase clinical drug development. The present study conducted pharmacokinetic/pharmacodynamic modeling analysis for sinogliatin in healthy subjects followed by population pharmacokinetic/pharmacodynamic analysis for sinogliatin in T2DM patients. Models A and B could capture the pharmacokinetic/pharmacodynamic characteristics of sinogliatin in healthy subjects and T2DM patients in a robust manner. On the basis of Models A and B, Model C successfully predicted the quantitative relationship between the SG level after short-term treatment and the HbA_{1c} level after mid-term treatment. Therefore, the present study establishes a solid foundation for future sinogliatin modeling analysis during phase II/III studies. Serum insulin, C-peptide, glucagon-like peptide-1, and glucagon were also determined in healthy subjects in both studies. However, insulin secretion increased in the lower dose range (0–10 mg) and decreased in the higher dose range (>10 mg). A similar phenomenon was also observed in a clinical study of

another glucose kinase activator [29], which may have been caused by the feedback function of decreased glucose in the higher dose range. The dose-dependent exposure–response relationship for other biomarkers exhibited similar characteristics. Although we utilized the most mechanistic and complex model, an integrated glucose–insulin–glucagon model, to fit these data, we have not captured this kind of characteristic so far [29]. Therefore, this type of characteristic makes it difficult to interpret the differences in these biomarkers between healthy subjects and patients. Finally, only glucose was utilized in this analysis to describe the pharmacodynamic characteristics of sinogliatin in order to increase the accuracy of translational prediction. So far, GKAs have not been approved by regulatory authorities and many same-in-class drugs are under preclinical or clinical development. Therefore, it is of particular value for other GKAs to potentially be assisted by a model-based drug development (MBDD) strategy.

5 Conclusions

In the present study, we proposed a new MBDD methodology, the learn–research–confirm cycle, to predict the pharmacokinetic/pharmacodynamic characteristics of the novel GKA sinogliatin in T2DM patients from pharmacokinetic/pharmacodynamic data of healthy subjects and to simulate it after mid-term treatment based on short-term treatment data. Careful modeling of pharmacokinetic/pharmacodynamic profiles for same-in-class drugs in both healthy subjects and T2DM patients was additionally useful in optimizing the model. For sinogliatin, these findings were used to scale values of drug-specific and system-specific parameters as well as to modify the model structure by adding circadian rhythm and food effect to the model. This step of the research was proved to be necessary in order to accurately predict pharmacodynamic profiles across difference modulation systems. The current methodology may prove useful for the early-phase drug development of other GKAs. It also offers a good example of how to predict pharmacokinetic/pharmacodynamic profiles in patients with complex system profiles on the basis of data from healthy subjects. At the same time, the results of the population pharmacokinetic/pharmacodynamic analysis could offer a solid basis for further modeling research relating to sinogliatin during future phase II/III trials.

Compliance with Ethical Standards

Funding The study was supported by Ministry of Science and Technology of the People's Republic of China (the '12th Five-year' National Key Technology R&D Program of China; No. 2012ZX09303006-002 and 2014ZX09101002-004), the National Natural Science Foundation of China (No. 81403013), and the Shanghai Science and Technology Committee (the Shanghai Technology Program, No. 15XD1520500).

Conflict of interest Yi Zhang, John Choi, and Li Chen are employees in HuaMedicine (Shanghai) Ltd.), the company developing HMS-5552. Dongyang Liu, Ji Jiang, Xuening Li, Dalong Zhu, Dawei Xiao, Yanhua Ding, Hongwei Fan and Pei Hu declare no conflicts of interest that might be are relevant to the contents of this manuscript.

References

1. Mager DE, Jusko WJ. Development of translational pharmacokinetic-pharmacodynamic models. Clin Pharmacol Ther. 2008;83:909–12.
2. Danhof M, de Lange EC, Della POE, et al. Mechanism-based pharmacokinetic-pharmacodynamic (PK-PD) modeling in translational drug research. Trends Pharmacol Sci. 2008;29:186–91.
3. Jonsson S, Henningsson A, Edholm M, et al. Role of modelling and simulation: a European regulatory perspective. Clin Pharmacokinet. 2012;51:69–76.
4. Kowalski KG, Olson S, Remmers AE, et al. Modeling and simulation to support dose selection and clinical development of SC-75416, a selective COX-2 inhibitor for the treatment of acute and chronic pain. Clin Pharmacol Ther. 2008;83:857–66.
5. Peng JZ, Denney WS, Musser BJ, et al. A semi-mechanistic model for the effects of a novel glucagon receptor antagonist on glucagon and the interaction between glucose, glucagon, and insulin applied to adaptive phase II design. AAPS J. 2014;16:1259–70.
6. Matschinsky FM. Assessing the potential of glucokinase activators in diabetes therapy. Nat Rev Drug Discov. 2009;8:399–416.
7. Bedoya FJ, Matschinsky FM, Shimizu T, et al. Differential regulation of glucokinase activity in pancreatic islets and liver of the rat. J Biol Chem. 1986;261:10760–4.
8. Grewal AS, Sekhon BS, Lather V. Recent updates on glucokinase activators for the treatment of type 2 diabetes mellitus. Mini Rev Med Chem. 2014;14:585–602.
9. Xu HR, Sheng L, Chen WL, et al. Safety, tolerability, pharmacokinetics, and pharmacodynamics of novel glucokinase activator HMS5552: results from a first-in-human single ascending dose study. Drug Des Devel Ther. 2016;10:1619–26.
10. D'Argenio DZ, Schumitzky A. A program package for simulation and parameter estimation in pharmacokinetic systems. Comput Programs Biomed. 1979;9:115–34.
11. Liu D, Yang H, Jiang J, et al. Pharmacokinetic and pharmacodynamic modeling analysis of intravenous esomeprazole in healthy volunteers. J Clin Pharmacol. 2016;56:816–26.
12. Bowen HF, Moorhouse JA. Glucose turnover and disposal in maturity-onset diabetes. J Clin Invest. 1973;52:3033–45.
13. Boden G, Chen X, Urbain JL. Evidence for a circadian rhythm of insulin sensitivity in patients with NIDDM caused by cyclic changes in hepatic glucose production. Diabetes. 1996;45:1044–50.
14. Landersdorfer CB, Jusko WJ. Pharmacokinetic/pharmacodynamic modelling in diabetes mellitus. Clin Pharmacokinet. 2008;47:417–48.
15. Lennernäs H. Intestinal permeability and its relevance for absorption and elimination. Xenobiotica. 2007;37:1015–51.
16. Du Bois D, Du Bois EF. A formula to estimate the approximate surface area if height and weight be known. 1916. Nutrition. 1989;5:303–311 **(discussion 312–313)**.

17. Green B, Duffull S. Caution when lean body weight is used as a size descriptor for obese subjects. Clin Pharmacol Ther. 2002;72:743–4.
18. Lindbom L, Pihlgren P, Jonsson EN. PsN-Toolkit–a collection of computer intensive statistical methods for non-linear mixed effect modeling using NONMEM. Comput Methods Programs Biomed. 2005;79:241–57.
19. Jonsson EN, Karlsson MO. Xpose–an S-PLUS based population pharmacokinetic/pharmacodynamic model building aid for NONMEM. Comput Methods Programs Biomed. 1999;58:51–64.
20. Efron B. Bootstrap methods: another look at the jackknife. Ann Stat. 1979;7:1–26.
21. Rohatagi S, Carrothers TJ, Jin J, et al. Model-based development of a PPARgamma agonist, rivoglitazone, to aid dose selection and optimize clinical trial designs. J Clin Pharmacol. 2008;48:1420–9.
22. Betts AM, Clark TH, Yang J, et al. The application of target information and preclinical pharmacokinetic/pharmacodynamic modeling in predicting clinical doses of a Dickkopf-1 antibody for osteoporosis. J Pharmacol Exp Ther. 2010;333:2–13.
23. Liu D, Ma X, Liu Y, et al. Quantitative prediction of human pharmacokinetics and pharmacodynamics of imigliptin, a novel DPP-4 inhibitor, using allometric scaling, IVIVE and PK/PD modeling methods. Eur J Pharm Sci. 2016;89:73–82.
24. Claret L, Zheng J, Mercier F, et al. Model-based prediction of progression-free survival in patients with first-line renal cell carcinoma using week 8 tumor size change from baseline. Cancer Chemother Pharmacol. 2016;78:605–10.
25. Wang Y, Zhu R, Xiao J, et al. Short-term efficacy reliably predicts long-term clinical benefit in rheumatoid arthritis clinical trials as demonstrated by model-based meta-analysis. J Clin Pharmacol. 2016;56:835–44.
26. Feng S, Shi J, Parrott N, et al. Combining 'bottom-up' and 'top-down' methods to assess ethnic difference in clearance: bitopertin as an example. Clin Pharmacokinet. 2016;55:823–32.
27. Jadhav PR, Cook J, Sinha V, et al. A proposal for scientific framework enabling specific population drug dosing recommendations. J Clin Pharmacol. 2015;55:1073–8.
28. Zager MG, Kozminski K, Pascual B, et al. Preclinical PK/PD modeling and human efficacious dose projection for a glucokinase activator in the treatment of diabetes. J Pharmacokinet Pharmacodyn. 2014;41:127–39.
29. Schneck KB, Zhang X, Bauer R, et al. Assessment of glycemic response to an oral glucokinase activator in a proof of concept study: application of a semi-mechanistic, integrated glucose-insulin-glucagon model. J Pharmacokinet Pharmacodyn. 2013;40:67–80.
30. Radziuk J, Pye S. Quantitation of basal endogenous glucose production in Type II diabetes: importance of the volume of distribution. Diabetologia. 2002;45:1053–84.
31. Hong J, Gu WQ, Zhang YF, et al. The interplay of insulin resistance and beta-cell dysfunction involves the development of type 2 diabetes in Chinese obeses. Endocrine. 2007;31:93–9.
32. Radziuk J, Pye S. Diurnal rhythm in endogenous glucose production is a major contributor to fasting hyperglycaemia in type 2 diabetes. Suprachiasmatic deficit or limit cycle behaviour. Diabetologia. 2006;49:1619–28.
33. Radziuk J, Pye S. Production and metabolic clearance of glucose under basal conditions in Type II (non-insulin-dependent) diabetes mellitus. Diabetologia. 2001;44:983–91.
34. Roge RM, Klim S, Kristensen NR, et al. Modeling of 24-hour glucose and insulin profiles in patients with type 2 diabetes mellitus treated with biphasic insulin aspart. J Clin Pharmacol. 2014;54:809–17.
35. Shapiro ET, Polonsky KS, Copinschi G, et al. Nocturnal elevation of glucose levels during fasting in noninsulin-dependent diabetes. J Clin Endocrinol Metab. 1991;72:444–54.
36. Dalla MC, Caumo A, Basu R, et al. Minimal model estimation of glucose absorption and insulin sensitivity from oral test: validation with a tracer method. Am J Physiol Endocrinol Metab. 2004;287:E637–43.
37. Dalla MC, Caumo A, Cobelli C. The oral glucose minimal model: estimation of insulin sensitivity from a meal test. IEEE Trans Biomed Eng. 2002;49:419–29.
38. Jauslin PM, Silber HE, Frey N, et al. An integrated glucose-insulin model to describe oral glucose tolerance test data in type 2 diabetics. J Clin Pharmacol. 2007;47:1244–55.
39. Martin J. Red blood cell physiology. Biomed Instrum Technol. 1995;29:150–1.
40. Matschinsky FM, Zelent B, Doliba N, et al. Glucokinase activators for diabetes therapy: May 2010 status report. Diabetes Care. 2011;34(Suppl 2):S236–43.